A COMPARISON OF RECIPROCATING SLIDING AT LOW LOADS AND SCRATCH TESTING FOR EVALUATION OF TiN (PVD) COATING

F. ZIVIC[a]*, M. BABIC[a], N. GRUJOVIC[b], S. MITROVIC[a], D. ADAMOVIC[a], G. FAVARO[c]

[a] *Tribology Laboratory, Faculty of Mechanical Engineering, Kragujevac, Serbia*
E-mail: *zivic@kg.ac.rs*; *babic@kg.ac.rs*; *boban@kg.ac.rs*
[b] *Center for Information Technologies, Faculty of Mechanical Engineering, Kragujevac, Serbia*
E-mail: *gruja@kg.ac.rs*
[c] *CSM Instruments, Switzerland*
E-mail: *gregory.favaro@csm-instruments.com*; *mihaela.caunii@csm-instruments.com*

ABSTRACT

Tribological behaviour of TiN coating deposited on high alloyed tool steel during scratch testing and linear reciprocating testing, at micro Newton loads in dry contact conditions, was investigated in this study. Influence of coating surface roughness on friction coefficient and wear life of TiN coating was studied. The results showed that TiN coating friction and wear behaviour are strongly dependent on its surface roughness. High roughness resulted in adhesive coating failure and higher penetration depth during scratching and lower friction coefficient and higher wear level during sliding. TiN coating with the lowest arithmetic mean deviation of the roughness profile, R_a, 0.01 µm, exhibited the best adhesion properties and the lowest wear level.

Keywords: TiN coating, scratch test, linear reciprocating test, coating roughness effects.

AIMS AND BACKGROUND

Hard TiN coatings have been widely used for many years, as protective and wear resistant coatings in different areas of application. It is a well-known fact that TiN coatings considerably increase the lifetime of the coated surface[1–5]. Reciprocating sliding tests at micro-loads enable additional understanding of the coating

---

* For correspondence.

behaviour. Phenomena like asperity interactions, elastic and plastic deformation of surface layers, tribological layers formation, 3rd body influences on sliding behaviour of TiN coatings are particularly important concerning microtribological processes in such a system[6]. Scratch testing has been efficiently applied for evaluation of coatings[7–10]. Another approach for assessment of coating characteristics is by monitoring the friction coefficient during contact[5]. Sliding with high contact load was mainly considered for evaluation of the coating wear life and material transfer tendency[3,11,12].

Influence of the coating surface roughness on its tribological behaviour has been studied by many authors[2,11]. High surface roughness, in general, produces high wear rates, increases material transfer tendency and promotes crack initiation resulting in decreased coating life. Mathematical modelling and simulation of scratch testing, in order to predict coating behaviour (crack initiation, crack patterns, crack propagation, etc.), can provide insight into influences of various parameters[13]. Within this study, 4 coating surface roughnesses of TiN deposited on high alloyed tool steel were investigated using scratch testing and reciprocating sliding tests at micro-level loads. The influence of the surface roughness on the coating adhesion and coating failure has been examined. Influence of sliding conditions (load and sliding speed) and coating surface roughness on coating life has been studied. Wear mechanisms during sliding were analysed.

EXPERIMENTAL

Materials. For experimental investigations presented in this paper, high alloyed tool steel with high toughness and hardness, denoted by C4750 according to JUS standard (DIN 17006 designation: X165CrMoV12) was selected as a substrate material. The chemical composition of the investigated steel is (in mass concentration of elements): 1.65% C, 0.30% Si, 0.30% Mn, max. 0.035% P, max. 0.035% S, 12.0% Cr, max. 0.25% Ni, 0.60% Mo, 0.10% V, 0.50% W. Sample plates made of DIN X165CrMoV12 steel with dimensions of $70 \times 40 \times 5$ mm were prepared as substrate material. Quenching in oil and stress relieving were realised before final machining by abrading. Prior to deposition, stainless steel samples were grinded in order to obtain different surface roughness. Different surface roughness was achieved simply by using different grain sizes in a wet grinding process.

TiN coatings were deposited by means of the arc physical vapour deposition (PVD) method using a PUSK-83 device. Coating deposition was performed at 450°C. Deposition time was 21 min with deposition speed of 6–7 min/µm. Coating micro-hardness was 2000 HV. Surface defects were not observed on the coating after deposition using optical microscopy. Obtained coating thickness was in a range of 3–4 µm, determined on samples cross-section by optical microscopy. 4 groups of TiN coating samples were prepared, each having different coating

surface roughness: $R_a = 0.01$ μm (denoted by TiN0.01 further in the text); $R_a = 0.09$ μm (denoted by TiN0.09); $R_a = 0.4$ μm (denoted by TiN0.4), and $R_a = 0.8$ μm (denoted by TiN0.8).

Scratch testing. The scratch test is commonly used for evaluation of the adhesive and cohesive strength of films. Observed failure events during scratching are related to coating detachment at the coating–substrate interface and considered as a measure of adhesion. Critical load (Lc) is the load at which a specific failure event occurred. The smallest load, Lc_1, is the first critical failure point and corresponds to the onset of cohesive failure (cracking failure). Lc_2 usually indicates coating spallation or detachment, crack opening and growth, and Lc_3 indicates total delamination or perforation of the coating[7,9,10].

A controlled scratch under the linear load increase condition was realised using a CSM scratch tester. The values of the critical loads were detected and recorded by the scratch tester, together with automatic recording of optical micrographs using the built-in optical microscope. Recorded data are used to quantify the adhesive properties of the observed coating. Normal force was constantly increased from initial value of 0.5 N to the maximum value of 100 N by loading rate of 100 N/min. Linear speed of the indenter was 10.05 mm/min. Rockwell diamond stylus indenter was used, with 50 μm tip radius. Scratch testing was performed in accordance with ASTM D7187 standard.

Sliding direction was set perpendicular to the direction of the final grinding of the coated surface. 3 scratch tests were performed for each of the samples. All experiments were performed under dry sliding conditions, at room temperature of 22°C. Optical micrographs of the samples were captured at the exact moments when critical load was achieved, automatically detected by the scratch tester. Change of normal force, friction force and penetration depth (PD) were monitored and constantly recorded during testing. Scratching was realised with diamond indenter, meaning that all deformation processes can be attributed to TiN coated steel samples. Prior to testing, each sample was thoroughly cleaned by alcohol, then cleaned in isopropyl alcohol, by staying in the solution for 60 min and afterwards dried in hot air. Samples were stored in a closed desiccator, prior to testing.

Tribological tests. Series of reciprocating sliding tests were carried out using a CSM nanotribometer (details of the device are given in Ref. 14). Sapphire ball of 1.5 mm diameter was used as a static contact element. Sapphire was chosen as a counterpart material due to its relative chemical inertness, while at the same time providing necessary resistance to wear.

The same flat rectangular samples used for scratching (DIN X165CrMoV12 steel with TiN coating; 4 different coating roughnesses) were used as moving contact element. Testing was done with 0.4 mm stroke (0.2 mm half amplitude) in dry

82

conditions and in air at 25°C temperature. Test duration was 40 000 cycles. One cycle is represented by distance of 2 strokes. 5 values of normal force were used (100, 250, 500, 750 and 1000 mN) at sliding speed of 10 mm/s. Friction coefficient was monitored, in order to determine coating behaviour during sliding. The wear life of observed TiN coating was determined as the number of cycles after which the coefficient of friction starts to sharply increase as per literature practice[3].

Prior to testing, each sample was thoroughly cleaned by ethyl alcohol, then cleaned in isopropyl alcohol, by staying in the solution for 60 min and dried in a hot air. Samples were stored in a desiccator, prior to testing. The repeatability of the results for replicate tests was satisfying (coefficient of variation of the friction coefficient values was under 3%).

RESULTS

Real time diagrams of the friction force, normal force and penetration depth, as a function of the sliding distance (scratching distance), obtained by the scratch tester are shown in Fig. 1. Typical scratch morphology images simultaneously recorded by the scratch tester are shown in Figs 2 and 3. It can be clearly seen that friction coefficient exhibit different behaviour depending on the observed surface
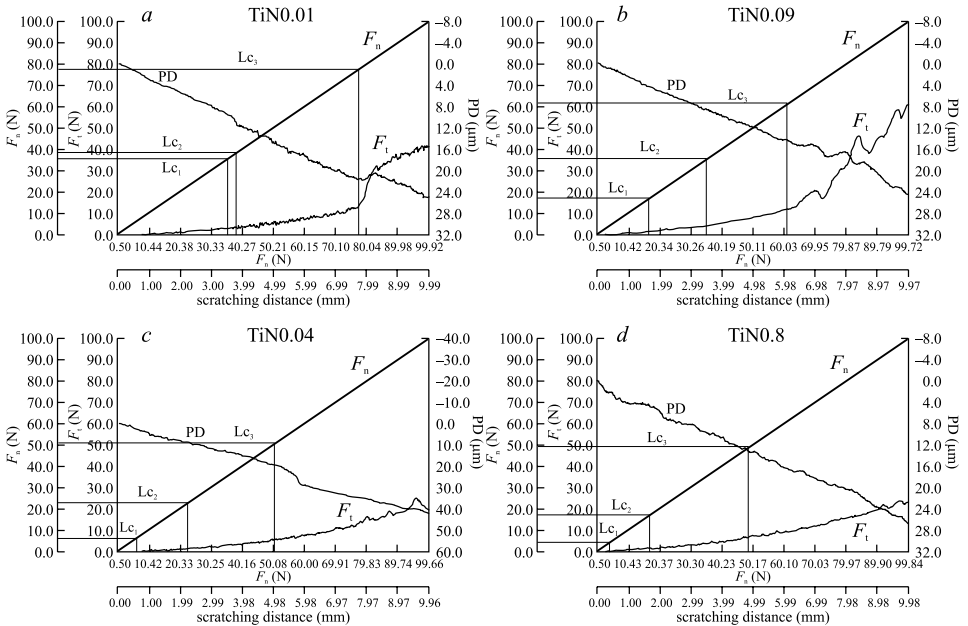

Fig. 1. Diagram of the friction force (F_t), normal force (F_n) and penetration depth (PD), during scratch testing as a function of the scratching distance: a – R_a = 0.01 μm, b – R_a = 0.09 μm, c – R_a = 0.4 μm, d – R_a = 0.8 μm

roughness. In case of the finest quality ($R_a = 0.01$ µm), friction coefficient curve proportionally rises with load increase up to the point when it sharply increased, indicating significant coating failure (Lc_3) (Fig. 1*a*). Similar behaviour can also be noticed for $R_a = 0.09$ µm, while in case of the high roughness ($R_a = 0.4$ µm and $R_a = 0.8$ µm) there was no abrupt changes of the friction coefficient like in previous cases (Fig. 1*c*, *d*).
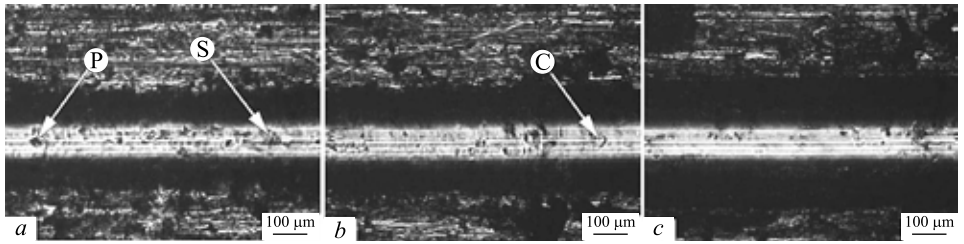
Optical micrographs of the scratching tracks at moments when Lc_1, Lc_2 and Lc_3 loads were detected are shown in Figs 2 and 3. Load Lc_1 (Figs 2*a*, 3*a*) corresponds to the appearance of the first visible failure of the coating (denoted by CD in Fig. 2*a*). Load Lc_2 (Figs 2*b* and 3*b*) indicates film spallation or detachment (denoted by CS in Fig. 2*b*), crack opening and growth (denoted by CO in Fig. 2*b*) and Lc_3 (Figs 2*c* and 3*c*) points to further extensive coating failure and total coating failure throughout large areas (denoted by S and CF in Fig. 2*c*). The other 2 coating roughnesses exhibited similar behaviour to those presented in Figs 2 and 3: TiN0.09 sample similar to TiN0.01 and TiN0.4 similar to TiN0.8.

It can be clearly seen (Fig. 2*a*) that in case of TiN0.01, the first visible coating failure occurred in a form of a coating delamination, in the central region of the track (denoted by CD in Fig. 2*a*) and also as coating chipping at the edge of the track (denoted by CC in Fig. 2*a*), what is in consistence with typical crack pattern reported by Holmberg et al.[15] Holmberg et al. showed that formation of cracks in the scratch groove can appear in several forms, whereat angular cracks appear first, leading to coating chipping at edges of the track. Coating spalling at the edge of the track can be clearly seen in Fig. 2*b* (denoted by CS). Also, transverse semi-circular cracks proved by Holmberg et al.[15] can be clearly observed in the central region of the track in Fig. 2*b* (denoted by CO). Exposed substrate can be seen in Fig. 2*c* (denoted by S and CF) indicating total coating failure under this load (Lc_3).

In case of TiN0.8 (Fig. 3*a*), surface cracks in the scratch groove, at Lc_1 load, is clearly characterised by appearance of number of small cracks, pits and grooves (denoted by P in Fig. 3*a*) in the central region quite different if compared to the previous case of fine roughness (Fig. 2*a*). Also, exposure of substrate along the
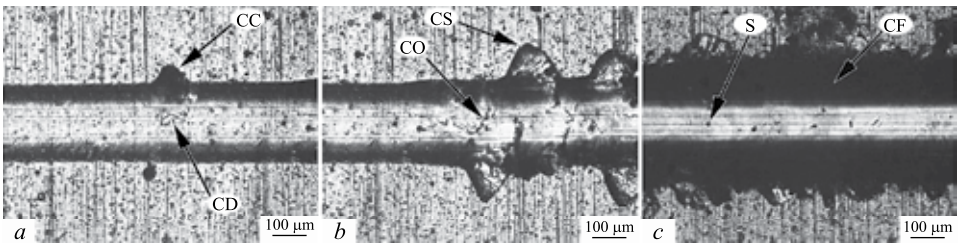
Fig. 2. Optical micrographs of the scratching scar (TiN0.01), at the position of the following critical load: *a* – Lc_1; *b* – Lc_2; *c* – Lc_3; (CC – coating chipping; CD – coating delamination; CO – crack opening; CS – spallation; S – exposed substrate; CF – total coating failure)

Fig. 3. Optical micrographs of the scratching scar (TiN0.8), at the position of the following critical load: a – Lc$_1$; b – Lc$_2$; c – Lc$_3$; (P – pits; S – exposure of substrate; C – semi-circular cracks)

scratching groove appeared already at the first critical Lc$_1$ load (denoted by S in Fig. 3a) on samples with higher roughness. Some forms of semi-circular cracks can be noticed in Fig. 3b (denoted by C), but unlike in previous case these cracks are not distinctly observed.

Evolution of the friction coefficient as a function of number of cycles, during linear reciprocating test, at 1000 mN load, is shown in Fig. 4. It can be clearly seen that friction coefficient during sliding of TiN0.01 sample (Fig. 4) exhibited typical frictional transition: the 1st period of the coating behaviour, e.g. wear life, the 2nd period of transition when coating failure occurred and the last period of total coating failure. This is in consistence with findings of Lee and Jeong[3] who reported the similar frictional behaviour during sliding (cone-on-disc) of TiN-coated steel samples against diamond. Results obtained in this study in case of high coating roughness also exhibited changes of friction coefficient over time but with much shorter initial periods of steady state values of friction coefficient. In case of high roughness (Fig. 4), transition period started earlier and total failure of the coating occurred earlier in comparison with fine roughness. There was no decrease of the friction coefficient after the coating failure, in case of high roughness, but only fluctuation of values until the end of the test. Similar behaviour was observed for other tested roughnesses: TiN0.09 similar to TiN0.01 and TiN0.4 similar to TiN0.8.

Dyrda and Sayer[7] reported that friction measurements alone are not absolutely reliable in precise determination of critical load for a coating and further determination of its wear life. Evolution of friction coefficient in our study exhibited 3 different periods in case of higher loads (Fig. 4). In case of lower loads (100, 250 mN), friction coefficient curve could be divided into 3 periods similar to those in Fig. 4, but with less pronounced differences in friction coefficient values over time. It is possible that with further decrease of the normal force, it would become hard to determine the precise moment of friction coefficient change that would represent the first coating failure. Results obtained by other authors[2,11] implies that in the case of TiN sliding contacts, there is the lack of 'running-in' behaviour, that is in consistence with our findings. It can be clearly seen that there was no

Fig. 4. Evolution of the friction coefficient during sliding as a function of number of cycles, Fn = 1000 mN: *a* – TiN0.01, *b* – TiN0.8
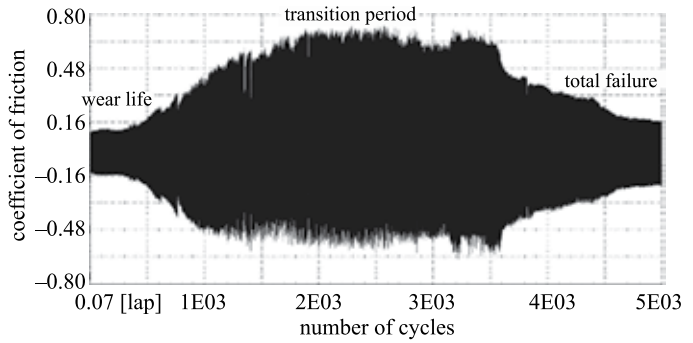
running-in period regarding friction coefficient curve in Fig. 4 and it was similar in all tests.

Optical micrographs of the worn track after sliding at 1000 mN load, after 10 000 cycles, are shown in Fig. 5. It can be clearly seen that wear mechanisms were different for TiN0.01 and TiN0.8 samples. In case of smooth coating surface (Fig. 5a), abrasive wear can be clearly observed and worn track was almost smooth, with no evidence of TiN particles. Coating delamination was not present
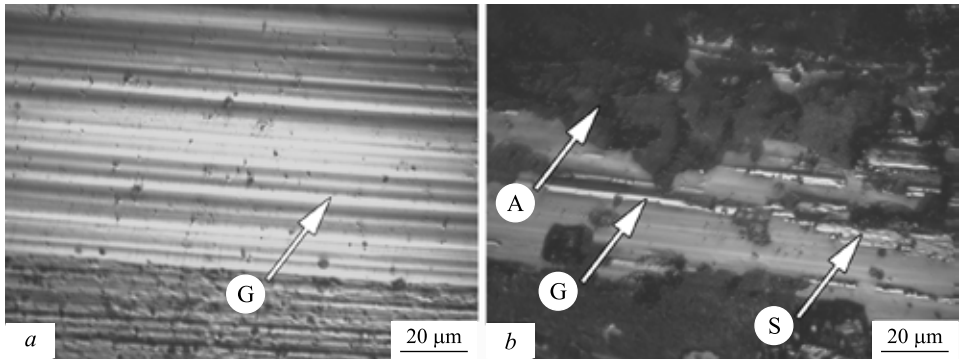
Fig. 5. Optical micrographs of the worn track after sliding: *a* – TiN0.01; *b* – TiN0.8; (G – groove; A – severe adhesive wear; S – spalling)

in case of TiN0.01 (Fig. 5a), as in case of TiN0.8 (Fig. 5b). Severe adhesive wear with deep abrasive grooves and delaminated areas can be clearly seen in Fig. 5b.

DISCUSSION

The obtained results showed that the critical loads during scratch testing were strongly influenced by the coating roughness. Values of Lc_1, Lc_2 and Lc_3 recorded by the scratch tester were used to determine the influence of the coating roughness on critical loads, as shown in Fig. 6. It can be noticed that the first

critical load, Lc_1 significantly decreased with roughness increase. Many studies have been devoted to identification of the first initiating crack in the coated surface[11,15]. The first formed crack further promotes more cracks and propagates the fast surface failure. According to Holmberg et al.[15], the first crack of TiN on steel starts at the edge of the scratch groove as angular crack. It is in consistence with results obtained in our study and appearance of the coating failure in angular direction at the edge of the scratching scar (denoted by CC in Fig. 2a).

Fig. 6. Influence of the coating roughness on coating adhesion

However, in case of high roughness, these typical crack patterns, as reported in literature, did not appear so obviously (such as in Fig. 3). It seems that the dominant wear mechanism is different for high and low roughness of the coating. Holmberg et al.[15] reported adhesive wear accompanied with extensive plastic deformation and fracture controlled wear during the scratching. According to Figs 3 and 5, it is obvious that high coating surface roughness resulted in early crack initiation, poor adhesion and increased coating spalling. Contact processes of surfaces are controlled by asperity interlocking, further breaking of generated bonds and asperity ploughing. According to Harlin et al.[11], high surface roughness of PVD coatings resulted in increased ploughing component of friction because of protruding surface asperities (macroparticles). Hard TiN particles of macro-size are generated on surface during asperity ploughing and breaking of adhesive bonds. Loose TiN particles further promote 3rd body abrasion and severe abrasive wear and coating spallation. It can be clearly seen that in case of TiN0.8 (Fig. 3), severe ploughing grooves, pits and microfracture of the coating occurred. Also, in case of TiN0.8, ridges along the scratch groove are much wider from the beginning of scratching if compared to TiN0.01 sample. Scratch damage mechanisms are obviously different for TiN0.01 and TiN0.8 samples (Figs 2 and 3).

It can be considered that TiN0.01 sample possesses good adhesion properties, because substrate material on the bottom of the track is only visible when the critical load $Lc_3 = 77.4$ N is achieved and no extensive delamination of the coating occurred before that load. Unlike samples with fine coating roughness that followed the typical development of the coating failure process, reported by Holmberg et al.[15], samples with high roughness (TiN0.4, TiN0.8) exhibited significant delamination of the coating just after the first critical load, Lc_1 (Fig. 3). Also, in case of TiN0.8, load Lc_1 was significantly lower if compared to TiN0.01

87
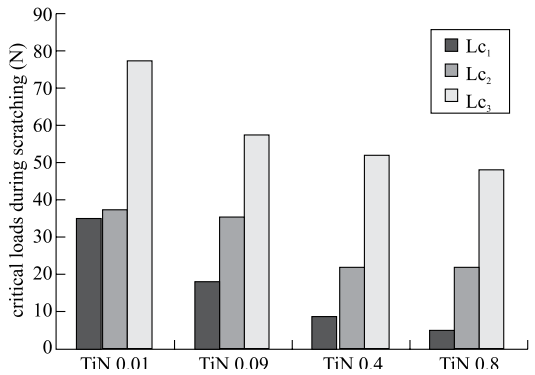
(Fig. 6). Friction force curve (Fig. 1c, d) exhibited oscillating trend after the first critical load Lc_1. This oscillating trend was not observed after the critical load Lc_3, in Fig. 1a, b. The friction coefficient sharply increased after reaching the critical load Lc_3, in case of fine roughness (Fig. 1a, b). This could be explained by the fact that, in case of fine roughness, coating delamination occurred in a few regions within a central area of the scratching track (Fig. 2), while for samples with high roughness, there was as a number of pits and delaminated areas throughout the scratch track (Fig. 3). This difference was obviously reflected in a friction coefficient behaviour. In case of TiN0.01 (Fig. 1a) and Ti0.09 (Fig. 1b), friction force curve abruptly increased several times, starting approximately from critical load Lc_3, whereas increase of the friction force is accompanied by decrease of the indenter penetration depth. This is a period of extensive coating delamination and total exposure of the substrate material. The material is plastically deformed, fractured and removed from the contact zone.

It is obvious that different coating failure modes were exhibited for smooth and rough surfaces: spalling failure (Fig. 2) and buckling or adhesive failure (Fig. 3). In case of TiN0.01 samples, coating damage and detachment mechanisms could be identified as: plastic deformation, crack formation, chip formation and flaking (Fig. 2). In case of TiN0.8, deformation and chip formation were not observed (Fig. 3). This difference could be explained by the evident poor adhesion that rough surfaces exhibited. Good adhesion of TiN0.01 sample influenced plastic deformation of the coating surface as the first response of the surface to the applied normal load. Later, angular cracks appeared first, leading to coating chipping at edges of the track. Only random flaking could be noticed (denoted by CD in Fig. 2a) since good coating adhesion prevented it from detachment. In case of TiN0.8 sample, applied force influenced occurrence of adhesive cracking along the scratch track, causing early exposure of the substrate (Fig. 3).

The obtained results of sliding tests showed that friction coefficient of TiN coating sliding against sapphire ball is influenced by the coating roughness and normal load, what is shown in Fig. 7a. Friction coefficient values (Fig. 7a), are mean values of dynamic friction coefficient in a period corresponding to the wear life of a coating (the 1st period of sliding, shown in Fig. 4). It can be clearly seen that friction coefficient values were increasing with load increase and decreasing with increase of the surface roughness (Fig. 7a), for all tested samples. This is in accordance with results of different authors that investigated influence of the coating roughness and contact load on friction coefficient[11,15]. Rough surfaces reduce the real contact. Higher values of surface roughness mean that smaller contact area would be realised between surfaces in relative contact, which in return results in lower tangential force and smaller friction coefficient. Harlin et al.[11] stressed out coating surface roughness as critical parameter in sliding contacts of TiN coatings, due to its lack of running-in behaviour. Holmberg et al.[15]

88

reported that high surface roughness promoted particle ploughing originating from loose particles or debris when present in sliding contact. At micro-level of loads, asperity tribology becomes of utmost importance for friction processes, because phenomena such as asperities adhesion and fracture, debris formation and changes in surface topography govern the friction process[15]. Achanta et al.[12] studied adhesion forces on rough and smooth TiN surface and reported that under micro-Newton loads surface roughness had no influence on recorded adhesion forces, due to formation of the native oxide layer. Also, rutile TiO_2 is produced during TiN sliding against sapphire[15]. It seems that even though protective oxide layers are formed on the surface (as proven by other authors), these layers were probably eliminated by hard TiN debris particles or not sufficiently present, in our study.

Fig. 7. Influence of the surface roughness and applied normal load during reciprocating sliding on: *a* – friction coefficient; *b* – coating life

Evaluation of the coating wear life during reciprocating sliding tests as the number of cycles is shown in Fig. 7*b*. As previously stated, wear life of a coating was calculated as a number of cycles during steady state friction (Fig. 4). Obtained trends in Fig. 7*b* are in accordance with results of Lee and Jeong[3]. It can be clearly seen (Fig. 7*b*) that increase of R_a produced more than several times decrease of coating life. It can be noticed that wear life of a coating decreased with load increase for all tested samples. TiN0.01 sample, under 100 and 250 mN load, was not destroyed even above the foreseen test limit of 40 000 cycles, compared to wear life of approximately 5000 cycles in case of rough coatings (TiN0.8).

Optical micrographs in Fig. 5 clearly show significantly different wear mechanisms for observed coatings. Severe adhesive wear, clearly seen in Fig. 5*b*, indicates that rough surface asperities promote strong adhesive bonds influencing extensive coating failure. Large delaminated areas in Fig. 5*b* throughout the worn track indicated further wear of the substrate material. Deep random abrasive grooves (Fig. 5*b*) indicated that worn TiN particles influenced a 3rd body abra-
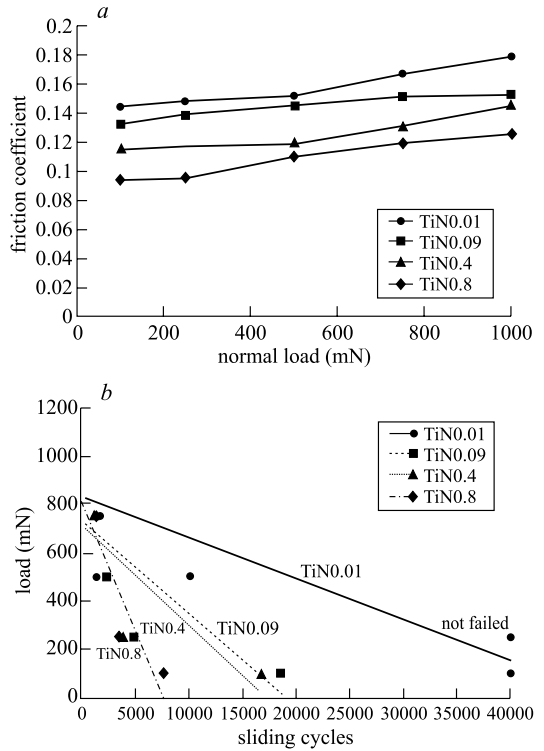
89

sion, additionally contributing to extensive wear. Since sapphire is significantly harder than TiN coating, third body abrasion can only originate from TiN particles. On the other hand, smooth coating surface minimise the maximum contact stresses on the asperity level and prevent severe ploughing of protruding asperities and generation of TiN particles. Almost smooth worn track with abrasive grooves can be observed in Fig. 5*a*. It is clear that smooth TiN0.01 sample did not exhibit 3rd body abrasion or any evidence of significant adhesive wear (Fig. 5*a*). Podgornik et al.[2] showed that rough coating surface increases material pick-up tendency, because surface irregularities and asperities represent sources which initiate material transfer. If debris generated by TiN coating is captured by the rougher topography, it results in ploughing and scratching, further promoting the wear rate. High surface roughness also promotes tendency to crack initiation and surface fatigue of the coating resulting from high contact stresses at the asperities[11]. If cyclic high contact stresses are present at asperities, fatigue resistance of the coating (resistance to crack initiation) is low, leading to crack propagation, fracture and high wear rate. Consequently, TiN0.8 sample exhibited more than 4 times shorter wear life (Fig. 7*b*) than TiN0.01, under low loads (100, 250 mN).

CONCLUSIONS

Scratch test results showed that critical loads decreased with surface roughness increase. They also showed that crack initiation, crack growth and crack pattern development in TiN coating, were different for high and low roughness. Higher penetration depth was achieved in case of high roughness of TiN coating. Coating failure analysis of the scratch test showed that spalling failure occurred in case of smooth surfaces and buckling (adhesive) failure was produced in case of high roughness.

Reciprocating sliding showed that mean friction coefficient increased with load increase and decreased with surface roughness increase. TiN coating wear life decreased significantly with increase of surface roughness. Friction coefficient behaviour of smooth surfaces at high normal loads during sliding exhibited sharp transitions with occurrence of the coating failure. These transitions became less pronounced with normal load decrease and with coating surface roughness increase. According to the obtained results in this study, it is possible to reliable determine coating life by observing friction coefficient behaviour, in case of smooth coatings and high normal loads. In case of low loads (100, 250 mN), it is necessary to perform sliding tests of longer duration and it is rather difficult to define the exact number of sliding cycles when the first coating failure occurred.

In case of high roughness, severe adhesive wear govern the wear behaviour of the TiN coating sliding against sapphire. In case of smooth surfaces, 3rd body abrasion, originating from TiN worn particles, had no influence on a wear behaviour and abrasive wear dominated with almost smooth worn tracks.

REFERENCES

1. C. LIU, Q. BI, A. MATTHEWS: Tribological and Electrochemical Performance of PVD TiN Coatings on the Femoral Head of Ti–6Al–4V Artificial Hip Joints. Surface and Coatings Technology, **163–164**, 597 (2003).
2. B. PODGORNIK, S. HOGMAR, O. SANDBERG: Influence of Surface Roughness and Coating Type on the Galling Properties of Coated Forming Tool Steel. Surface and Coatings Technology, **184**, 338 (2004).
3. Y. Z. LEE, K. H. JEONG: Wear-life Diagram of TiN-coated Steels. Wear, **217**, 175 (1998).
4. D. KAKAS, B. SKORIC, S. MITROVIC, M. BABIC, P. TEREK, A. MILETIC, M. VILOTIC: Influence of Load and Sliding Speed on Friction Coefficient of IBAD Deposited TiN. Tribology in Industry, **31**, 3 (2009).
5. D. ADAMOVIC, M. STEFANOVIC, M. ZIVKOVIC, F. ZIVIC: Investigation of Influence of Tribological Conditions on Friction Coefficient during Multiphase Ironing for Steel and Aluminium Sheet Metal. Tribology in Industry, **28**, 29 (2006).
6. P. E. KRAJEWSKI, A. T. MORALES: Tribological Issues during Quick Plastic Forming. J. of Materials Engineering and Performance, **13**, 700 (2004).
7. K. DYRDA, M. SAYER: Critical Loads and Effective Frictional Force Measurements in the Industrial Scratch Testing of TiN on M2 Tool Steel. Thin Solid Films, **355–356**, 277 (1999).
8. S. J. BULL, E. G. BERASETEGUI: An Overview of the Potential of Quantitative Coating Adhesion Measurement by Scratch Testing. Tribology Internationl, **39**, 99 (2006).
9. P. J. BURNETT, D. S. RICKERBY: The Relationship between Hardness and Scratch Adhesion. Thin Solid Films, **154**, 403 (1987).
10. P. J. BURNETT, D. S. RICKERBY: The Scratch Adhesion Test: An Elastic-plastic Indentation Analysis. Thin Solid Films, **157**, 233 (1988).
11. P. HARLIN, P. CARLSSON, U. BEXELL, M. OLSSON: Influence of Surface Roughness of PVD Coatings on Tribological Performance in Sliding Contacts. Surface and Coatings Technology, **201**, 4253 (2006).
12. S. ACHANTA, D. DREES, J. P. CELIS: Investigation of Friction on Hard Homogeneous Coatings during Reciprocating Tests at micro-Newton Normal Forces. Wear, **263**, 1390 (2007).
13. V. JAYARAM, S. BHOWMICK, Z.-H. XIE, S. MATH, M. HOFFMAN, S. K. BISWAS: Contact Deformation of TiN Coatings on Metallic Substrates. Materials Science and Engineering A, Structural Materials, **423**, 8 (2006).
14. F. ZIVIC, M. BABIC, I. CVIJOVIC-ALAGIC, S. MITROVIC, A. VENCL: Wear Behaviour of Ti6Al4V Alloy against Al_2O_3 under Linear Reciprocating Sliding. J. of the Balkan Tribological Association, **17**, 27 (2011).
15. K. HOLMBERG, H. RONKAINEN, A. LAUKKANEN, K. WALLIN: Friction and Wear of Coated Surfaces – Scales, Modelling and Simulation of Tribomechanisms. Surface and Coatings Technology, **202**, 1034 (2007).